NACA

RESEARCH MEMORANDUM

OBSERVATION OF LAMINAR FLOW ON A BLUNTED 15° CONE-CYLINDER IN FREE FLIGHT AT HIGH REYNOLDS NUMBERS AND FREE-STREAM MACH NUMBERS TO 8.17

By John H. Disher and Leonard Rabb

Lewis Flight Propulsion Laboratory
Cleveland, Ohio

NATIONAL ADVISORY COMMITTEE
FOR AERONAUTICS

WASHINGTON

October 15, 1956

NATIONAL ADVISORY COMMITTEE FOR AERONAUTICS

RESEARCH MEMORANDUM

OBSERVATION OF LAMINAR FLOW ON A BLUNTED 15° CONE-CYLINDER IN FREE FLIGHT AT HIGH REYNOLDS NUMBERS AND FREE-STREAM MACH NUMBERS TO 8.17

By John H. Disher and Leonard Rabb

SUMMARY

A highly polished 15° included-angle cone-cylinder with hemispherical tip has been flown in order to obtain boundary-layer transition and heat-transfer data. The model was launched from a carrier airplane at an altitude of 47,500 feet and reached a maximum Mach number of 8.17 at an altitude of 37,500 feet. When at peak Mach number, laminar flow existed at the most aft measuring stations on the cone and cylinder surfaces. The Reynolds numbers at these stations were 35.2×10^6 and 38.5×10^6 for the cone and cylinder, respectively.

The results of this flight indicate the appreciable and favorable effect of tip bluntness in raising the allowable skin temperature for a given boundary-layer transition Reynolds number.

INTRODUCTION

The need for experimental data on heat transfer and boundary-layer transition at high Mach numbers is well recognized. Much of the needed data must be obtained by actual flight tests because existing ground facilities do not provide the combinations of high Mach number, high Reynolds number, and high total temperature which must be investigated.

In earlier flight tests (refs. 1 to 3), heat-transfer and transition data were obtained on a sharp-pointed 20° cone-cylinder at Mach numbers up to 5.18. In order to extend the Mach number range of the investigation, a new research vehicle has been designed and one model has been flown. The vehicle was launched from a jet airplane at high altitude and was propelled to high Mach numbers by two stages of solid propellant rocket. Data on boundary-layer transition, heat transfer, and drag from this flight are herein presented.

[redacted]

APPARATUS AND PROCEDURE

A sketch of the model is shown in figure 1. The model forebody consisted of a 15° included-angle cone with a 6-inch-diameter base. The tip of the cone was rounded to a 7/16-inch radius. The first 2.2 inches of the forebody were solid SAE 1020 steel. Aft of this point, the cone skin was made of 0.062-inch (nominal) Inconel (actual skin thickness is indicated on fig. 1 for each station). The conical forebody was attached to an Inconel cylinder 42 inches long. The aft 10 inches of the model formed a 9°50' half-angle flared skirt. The cylinder and flared skirt were formed of 1/32-inch (nominal) Inconel. Small wedge-shaped fins were attached to the flared skirt. These fins were fabricated from 1/32-inch Inconel, and the leading edges were cooled with internally inlaid solid-copper strips. The flared skirt was supported by a balsa-wood insert. The nose cone and instrumented portion of the cylinder (fig. 2) were highly polished to a surface finish of the order of 2 microinch rms. The aft portion of the cylinder and the flared skirt were chemically blackened to increase their emissivity and thus reduce peak skin temperature on these surfaces. The model carried 3 pounds of brass ballast which was located immediately behind the solid steel tip. The weight of the model without booster was 80.2 pounds, and the center of gravity was 40.2 inches back from the model tip.

The instrumentation carried within the model consisted of two axial accelerometers, two resistance-wire skin-temperature pickups, and four skin-temperature thermocouples. All temperature pickups were attached to the inner surface of the skin. One of the thermocouples and one of the resistance elements failed prior to launching.

The location of the usable skin-temperature pickups and the ranges of all the instruments are shown in the following table:

Quantity	Location	Range
Axial acceleration		1 to -25 g's
Axial acceleration		0 to 90 g's
Skin temp. (thermocouple)	Station 9.75	300° to 1600° R
Skin temp. (thermocouple)	Station 14.45	300° to 1600° R
Skin temp. (thermocouple)	Station 21.75	300° to 1600° R
Skin temp. (resistance wire)	Station 29.50	300° to 1500° R

The acceleration and resistance-wire temperature measurements were continuous while the thermocouple measurements were switched in such a manner that each temperature was recorded at about 0.07-second intervals. The measurements were telemetered to a ground receiving station. The small solid Inconel fins visible in figure 1 served as the transmitting antenna.

[redacted]

The model was propelled by a T40 rocket booster assembly and by a T55 rocket carried within the cylindrical and flared parts of the model. A photograph of the complete model and booster assembly is shown in figure 3. The booster structure consisted of an aluminum tube with a wall thickness of 1/16 inch and with cruciform aluminum fins mounted at the rear. The fins were 1/4 inch thick, with the leading edges tapered and rounded to a 1/16-inch radius. The booster rocket was maintained at a temperature of 100° F prior to firing by an electric blanket mounted between the rocket and the booster shell.

The booster assembly, which was locked to the model by a frangible disk coupling, was released upon firing of the T55 rocket. The weight of the booster and coupling assembly was 159 pounds.

The vehicle was carried aloft on a F2H-2B airplane, as shown in figure 4, and was launched in level flight at an absolute altitude above sea level of 47,500 feet. The booster and sustainer rockets were fired at 5.4 and 11 seconds, respectively, after release by delay squibs which were energized as the model left the launcher. During rocket burning, the model was tracked from the ground by radar and phototheodolite equipment. After rocket burnout, the model was not visible and was tracked only by radar.

A detailed discussion of the calculation procedure used is given in reference 2. The velocity of the model for this flight was determined from radar measurements and by integrating the acceleration data. The altitude was determined from radar measurements; the variation of free-stream static pressure and temperature with altitude was determined from a radiosonde survey made immediately following the flight. In calculating heat-transfer coefficients for stations 9.75 and 14.45, the temperature gradient through the skin was accounted for. This effect was negligible for stations 21.75 and 29.50. Conduction along the skin was negligible in all cases.

In reference 4 it is shown that tip bluntness lowers the Mach number and Reynolds number of an annulus of air about the body. If this annulus of low Reynolds number air is large enough to blanket the boundary layer, it is argued that the lower Reynolds number and Mach number determine the boundary-layer behavior. For comparison, the conditions outside the boundary layer at the various stations were calculated herein with and without the effects of tip bluntness considered. With bluntness effects neglected, the conditions are designated by subscript ∞ and are referred to as "sharp-tip conditions"; calculations were based on the tabulated values given in references 5 and 6 for sharp-tipped cone-cylinders. Blunt-tip conditions are designated by subscript δ; these conditions were calculated by assuming that a normal-shock total-pressure loss occurs and that the surface static pressure at the temperature measuring stations is unaffected by bluntness.

[redacted]

The Reynolds numbers at the various stations were computed for both blunt-tip and sharp-tip conditions on the basis of actual surface distances from the stagnation point of the model. These distances are shown in the following table:

Station	Surface distance, in.
9.75	10.1 (0.84 ft)
14.45	14.84 (1.24 ft)
20.00 (Cone-cylinder shoulder)	20.48 (1.71 ft)
21.75	22.21 (1.85 ft)
29.50	29.96 (2.50 ft)

The error in determing the free-stream Mach number M_0 for this flight is estimated to be within $\pm 2\frac{1}{2}$ percent of M_0 or ± 0.10, whichever is greater; and the error in measuring skin temperature is estimated to be within ± 2 percent of the full-scale range of the instrument or $\pm 25^\circ$ F.

RESULTS AND DISCUSSION

Free-Stream Conditions

A time history of free-stream Mach number is presented in figure 5. The model was launched at a free-stream Mach number of 0.67, fell freely until booster ignition at 5.4 seconds, and then accelerated to a maximum free-stream Mach number of 8.17 at 12.8 seconds after release. After rocket burnout, the model decelerated to a Mach number of 1.0 in about 15 seconds; thereafter the Mach number was subsonic. Maximum acceleration of 82 g's and maximum deceleration of 22.4 g's occurred at 12.2 and 14.5 seconds, respectively.

A plot of absolute altitude above sea level against time is presented in figure 6. The peak Mach number was reached at an altitude of 37,500 feet, and the model reached sea level 61 seconds after release.

The variation of free-stream static pressure with time is presented in figure 7, and the variation of free-stream Reynolds number per foot with time is presented in figure 8. At peak Mach number, the free-stream Reynolds number per foot was approximately 18×10^6. The maximum model Reynolds number was thus 108×10^6 based on a length of 71.7 inches.

[redacted]

Conditions at Outer Edge of Boundary Layer

A time history of the Mach number and the Reynolds number per foot outside the boundary layer at the temperature measuring stations is shown in figures 9 and 10, respectively. The Mach number for sharp-tip conditions M_∞ is shown in figure 9(a). The values for stations 21.75 and 29.50 are higher than the free-stream values (fig. 5) because of the overexpansion around the cone-cylinder junction. The Mach numbers for blunt-tip conditions M_δ are shown in figure 9(b). The Mach numbers are, or course, reduced appreciably because of bluntness, with the maximum value for station 21.75 reduced to 3.80.

The Reynolds number per foot for sharp-tip conditions (Re_∞ per ft) is shown in figure 10(a). The values at stations 21.75 and 29.50 are lower than the free-stream values (fig. 8) because of the overexpansion at the cone-cylinder junction. The maximum cone Reynolds number per foot was 28.4×10^6, resulting in a maximum cone Reynolds number of 48.5×10^6 based on a length of 20.48 inches. The Reynolds number per foot for blunt-tip conditions (Re_δ per ft) is shown in figure 10(b). With bluntness effects considered, the maximum Reynolds number per foot for the cone is reduced to 6.25×10^6. The maximum number occurs at about 22 seconds when the model has decelerated to a free-stream Mach number of 2.3.

Drag

A curve of the total drag coefficient for the sustainer stage (2^{nd} stage) of the model is presented in figure 11. The reference area is 0.196 square foot, which corresponds to the 6-inch-diameter cylinder. The drag was obtained from deceleration data during the coast period. The drag coefficient increased from about 0.30 at M_0 of 7.0 to about 1.2 at M_0 between 1.5 and 1.2. The portion of the curve above M_0 of about 7.0 is inaccurate due to the effects of rocket thrust decay. The relatively high drag coefficients are due to the large flared base. During acceleration, the total drag was appreciably lower because the rocket jet eliminated the base drag.

Temperatures and Heat-Transfer Coefficients

Time histories of the measured skin temperatures are shown in figure 12. Also presented are the free-stream total temperature, the adiabatic wall temperature for laminar or turbulent flow, and the free-stream static temperature. In comparing the skin-temperature histories, it should be remembered that the skin thickness of the cylinder is half that of the cone. The temperature at station 29.50 is noted to undergo

an abrupt change in slope at 19.5 seconds. This indicates transition from laminar to turbulent flow. The change in slope is more apparent in figure 13, where the skin temperatures are plotted to a larger scale.

Heat-transfer coefficients calculated from the temperature-time curves are shown in figure 14. Also shown are theoretical laminar and turbulent heat-transfer coefficients from references 7 and 8, respectively. For theoretical turbulent values, the Stanton number was assumed to equal 0.6 times the friction coefficient. The theoretical and experimental values shown are for blunt-tip conditions. The effect of the flow expansion around the cone-cylinder junction on the theoretical laminar heat-transfer coefficients at stations 21.75 and 29.50 was calculated by the method suggested in reference 9. For turbulent flow, the theoretical values at stations 21.75 and 29.50 were based on flat-plate values with the Reynolds number arbitrarily based on distance from the tip.

The experimental heat-transfer coefficients vary smoothly with time until 19.6 seconds for station 29.50 and about 20.0 seconds for stations 9.75, 14.45, and 21.75. The abrupt rise of heat-transfer coefficient at these times is assumed to indicate transition from laminar to turbulent flow. Heat-transfer coefficients cannot be calculated with any degree of accuracy between about 20 and 23 seconds because of the very small difference between wall and recovery temperatures. Experimental values after 23 seconds are of turbulent magnitude. During the period between about 14 seconds and transition, the experimental values are appreciably higher than laminar theory, whereas prior to 14 seconds fair agreement exists. This may be partially explained by considering the effects of axial temperature gradients. The theoretical values shown are for zero temperature gradient along the model. This condition is approximately satisfied during the first 14 seconds. Later in the flight, an appreciable temperature gradient exists along the shell. Correction to the theory for the temperature gradient on the model would increase the theoretical values and thus would tend to produce closer agreement with experiment; however, inasmuch as the temperature distribution on the model forward of station 9.75 was not measured, quantitative temperature-gradient effects can not be calculated.

Transition Conditions

Boundary-layer instability and boundary-layer transition are not synonymous; however, boundary-layer transition from laminar to turbulent flow may be a consequence of boundary-layer instability. Therefore, a comparison of the measured transition conditions of this flight and the predictions of the stability theory is indicated. This comparison is made in figure 15. The theoretical solution shown is that of reference 10. Theory states that temperature ratios below the theoretical curve

result in complete boundary-layer stabilization for two-dimensional disturbances. Also shown in figure 15 is a single theoretical point at a Mach number of 4.0 based on three-dimensional disturbances (ref. 10). This solution indicates that stability for three-dimensional disturbances may be attainable at Reynolds numbers on the order of 10^{12} at a temperature ratio slightly less than that required for infinite stability for two-dimensional disturbances.

The data in figure 15 are presented for both sharp-tip and blunt-tip conditions. If sharp-tip conditions are used, much of the laminar region of the trajectory lies outside the theoretical stability curve. If blunt-tip conditions are used, much of the laminar region of the flight lies within the theoretical stability curve. The favorable effect of blunt tip on the theoretical stability margin is most pronounced near the peak Mach number, where a theoretically unstable condition is transformed into a condition of substantial stability margin. For sharp-tip conditions, laminar flow existed at Reynolds numbers greater than 38.5×10^6 on the cylinder (station 29.50) and 35.2×10^6 on the cone (station 14.45) at a free-stream Mach number of 8.17. Inasmuch as the boundary layer was laminar at stations 14.45 and 21.75 for much of the flight, it is possible that the flow was laminar at station 20.00, the end of the cone. If this is assumed to be true, then it can be said that laminar flow existed at a Reynolds number greater than 48.6×10^6 (based on sharp-tip conditions) at a free-stream Mach number of 8.17. The temperature ratios at maximum Reynolds number were 0.96 for the cone and 1.36 for the cylinder.

When transition occurred at station 29.50, the Reynolds number (sharp-tip conditions) was 27.5×10^6, the local Mach number was 3.60, and the temperature ratio was 1.92. For stations 9.75, 14.45, and 21.75, the transition Reynolds number varied from 10.75×10^6 to 18.5×10^6 while the local Mach number varied from 3.0 to 3.40.

When the effects of blunting are included, the Reynolds numbers at transition are higher than the Reynolds numbers at peak free-stream Mach number (see fig. 10(b)). The blunt-tip conditions at transition for station 29.50 were a local Mach number of 2.52, a local Reynolds number of 11.1×10^6, and a temperature ratio of 1.23.

At station 21.75 the Mach number at transition is the same as for station 29.50 and the Reynolds number is somewhat lower. However, the temperature ratio at station 21.75 is appreciably higher. This higher temperature ratio at transition is attributed to a stabilizing effect of the expansion at the cone-cylinder junction on the boundary layer in this region. Because of this strong pressure gradient, the transition conditions at station 21.75 can not validly be compared with the theory, which assumed zero pressure gradient.

[redacted]

For the cone (stations 14.45 and 9.75) the temperature ratios at transition are comparable with that at station 21.75, but the Mach number and Reynolds number are somewhat lower. The Reynolds numbers, Mach numbers, and temperature ratios at which transition occurred are summarized in table I for the two methods of computation. Also shown are the values for these parameters at maximum free-stream Mach number.

Figure 16 shows a comparison of the transition conditions of this flight with previously obtained flight data (ref. 3) and wind-tunnel results (ref. 11) for sharp-tipped models. Temperature ratio is plotted against Reynolds number at transition.

It is apparent that better agreement with previous results is obtained when blunt-tip conditions are used in the calculations for the present model. This implies that for the conditions of figure 16 the blunt properties are controlling and that for the same length of laminar run the wall temperature with a blunt-tipped model could be higher than the wall temperature of a sharp-tipped model by a factor of t_δ/t_∞, where t is local static temperature.

The theoretical stability solutions shown in figure 15 indicate an appreciable decrease in the temperature ratio for infinite stability with decreasing Mach number at Mach numbers less than about 4.00. However, in the previously obtained results (refs. 3 and 11) shown in figure 16, the value of temperature ratio at which the transition Reynolds number tends toward infinity was found to vary only slightly within the local Mach number range from 2.68 to 3.92. For blunt-tip conditions, the present results cover a Mach number range from 2.15 to 2.52, and within the scatter of the data no Mach number effect is discernible. If the theoretical variation with Mach number of the allowable temperature ratio for infinite boundary-layer stability were to be realized, the tip-bluntness effect on allowable wall temperature for a given length of laminar run would be altered appreciably.

For the blunt-tip conditions, both transition points for the cone are at low Reynolds numbers, where the values of temperature ratio are higher than the asymptotic value. Only station 29.50 with the transition Reynolds number of 11.1×10^6 is on the flat part of the curve, and thus only the transition conditions for station 29.50 can be compared with stability theory. As noted previously (fig. 15(d)), the transition conditions for station 29.50 agreed closely with the theoretical infinite stability boundary. The slight adverse pressure gradient at station 29.50 apparently has had no distinguishable effect on transition.

SUMMARY OF RESULTS

A highly polished 15° included-angle cone-cylinder with hemispherical tip has been flown to obtain boundary-layer transition data at high Mach numbers. The following results have been obtained:

1. A maximum free-stream Mach number of 8.17 and maximum local Reynolds number on the cone of 48.5×10^6 (based on sharp-tip conditions) were reached during the flight.

2. Laminar flow existed at Reynolds numbers (based on sharp-tip conditions) greater than 35.2×10^6 on the cone and greater than 38.5×10^6 on the cylinder when the model was at peak Mach number.

3. Transition from laminar to turbulent flow occurred for the most aft station on the cylinder when the model had decelerated to a free-stream Mach number of 3.45 and the temperature ratio had risen to 1.92. The Reynolds number at this time was 27.5×10^6.

4. The results of this flight, when compared with previous results for a sharp-tipped model, indicated appreciable favorable effect of tip bluntness in raising the allowable skin temperature for a given boundary-layer transition Reynolds number.

5. When laminar flow existed on the model and when temperature gradients along the model were small, the experimental heat-transfer data showed fair agreement with laminar theory. When appreciable temperature gradients existed, the experimental data were higher than the laminar theory.

Lewis Flight Propulsion Laboratory
National Advisory Committee for Aeronautics
Cleveland, Ohio, August 1, 1956

REFERENCES

1. Messing, Wesley E., Rabb, Leonard, and Disher, John H.: Preliminary Drag and Heat-Transfer Data Obtained from Air-Launched Cone-Cylinder Test Vehicle over Mach Number Range from 1.5 to 5.18. NACA RM E53I04, 1953.

2. Rabb, Leonard, and Simpkinson, Scott H.: Free-Flight Heat-Transfer Measurements on Two 20°-Cone-Cylinders at Mach Numbers from 1.3 to 4.9. NACA RM E55F27, 1955.

3. Rabb, Leonard, and Disher, John H.: Boundary-Layer Transition at High Reynolds Numbers as Obtained in Flight of a 20° Cone-Cylinder with Wall to Local Stream Temperature Ratios Near 1.0. NACA RM E55I15, 1955.

4. Moeckel, W. E.: Some Effects of Bluntness on Boundary-Layer Transition and Heat Transfer at Supersonic Speeds. NACA TN 3653, 1956.

5. The Staff of the Computing Section Center of Analysis: Tables of Supersonic Flow Around Cones. Tech. Rep. No. 1, M.I.T., 1947. (Contract NOrd 9169.)

6. Clippinger, R. F., Giese, J. H., and Carter, W. C.: Tables of Supersonic Flows About Cone Cylinders. Pt. I: Surface Data. Rep. No. 729, Ballistic Res. Labs., Aberdeen Proving Ground (Md.), July 1950. (Proj. TB3-0108H of Res. and Dev. Div., Ord. Dept.)

7. Van Driest, E. R.: Investigation of Laminar Boundary Layer in Compressible Fluids Using the Crocco Method. NACA TN 2597, 1952.

8. Van Driest, E. R.: Turbulent Boundary Layer in Compressible Fluids. Jour. Aero. Sci., vol. 18, no. 3, Mar. 1951, pp. 145-161.

9. Jack, John R., and Diaconis, N. S.: Heat-Transfer Measurements on Two Bodies of Revolution at a Mach Number of 3.12. NACA TN 3776, 1956.

10. Dunn, D. W., and Lin, C. C.: On the Stability of the Laminar Boundary Layer in a Compressible Fluid. Jour. Aero. Sci., vol. 22, no. 7, July 1955, pp. 455-477.

11. Jack, John R., and Diaconis, N. S.: Variation of Boundary-Layer Transition with Heat Transfer on Two Bodies of Revolution at a Mach Number of 3.12. NACA TN 3562, 1955.

[redacted]

TABLE I. - TRANSITION CONDITIONS AND CONDITIONS AT MAXIMUM FREE-STREAM MACH NUMBER

Station	Mach number at transition		Reynolds number at transition		Temperature ratio at transition		Maximum Mach number (a)		Reynolds number at maximum Mach number (a)		Temperature ratio at maximum Mach number (a)	
	Sharp tip	Blunt tip	Sharp tip	Blunt tip	Sharp tip	Blunt tip	Sharp tip	Blunt tip	Sharp tip	Blunt tip	Sharp tip	Blunt tip
9.75	3.0	2.15	10.75×10^6	4.75×10^6	2.35	1.62	6.85	2.87	23.9×10^6	2.03×10^6	1.00	0.25
14.45	3.0	2.15	15.9	7.0	2.19	1.51	6.85	2.87	35.2	3.00	.96	.25
20.00	---	----	---------	--------	----	----	[b]6.85	[b]2.87	[b]48.6	[b]4.14	----	----
21.75	3.4	2.52	18.5	8.4	2.40	1.65	8.50	3.80	27.4	2.22	1.34	.34
29.50	3.60	2.52	27.5	11.1	1.92	1.26	8.38	3.78	38.5	3.25	1.36	.35

[a]Laminar flow existed.

[b]Laminar flow assumed to exist.

Station, in.	Actual skin thickness, in.
9.75	0.0591
14.45	.0589
21.75	.0305
29.50	.0310

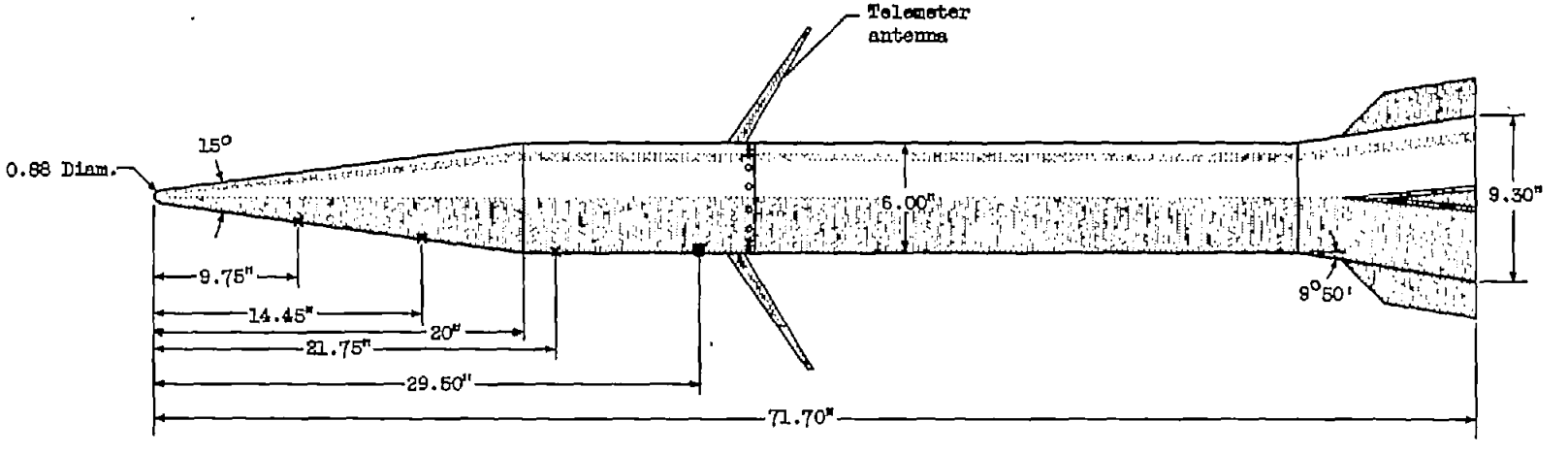

Figure 1. - Dimensions of model.

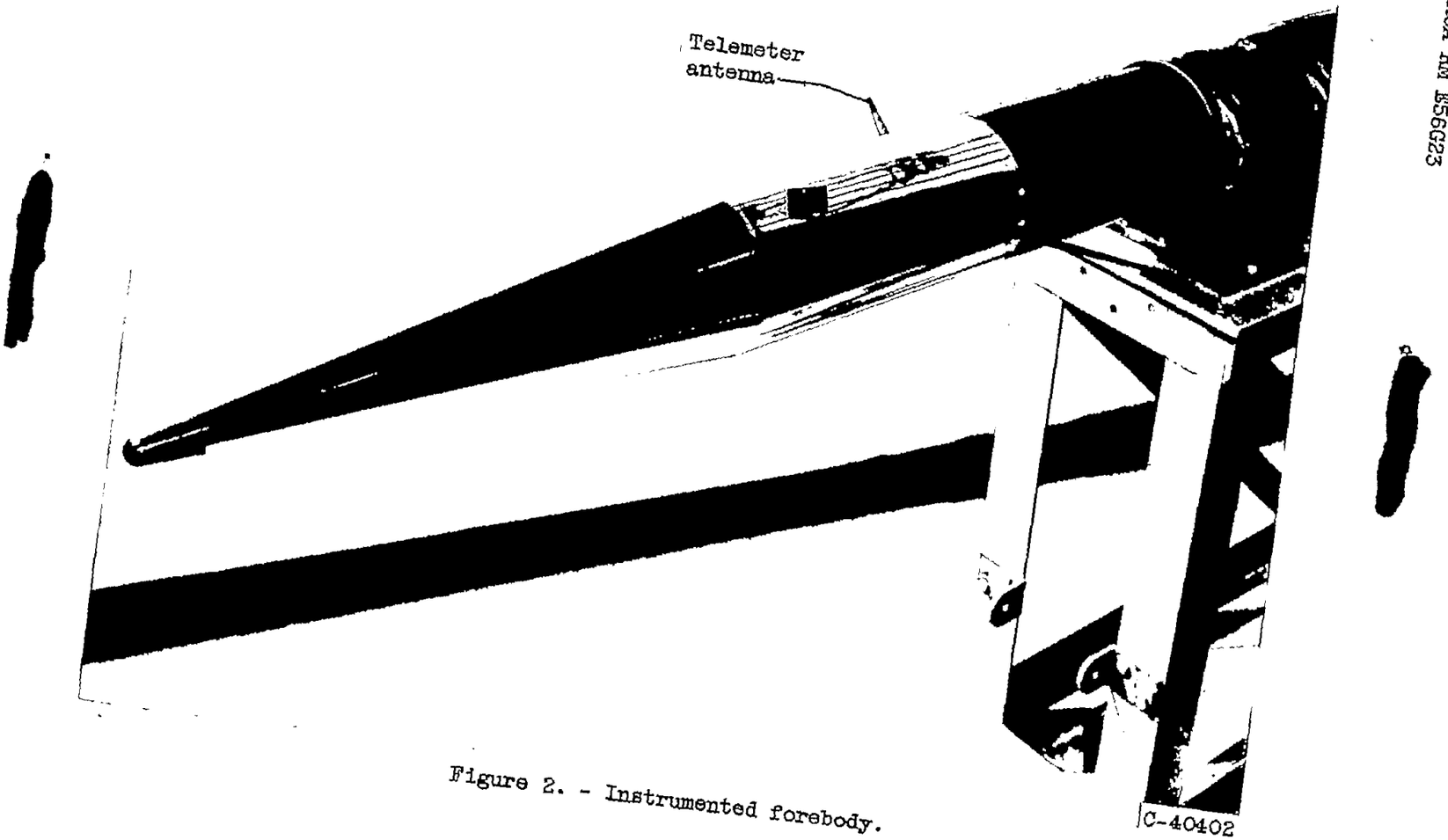

Figure 2. - Instrumented forebody.

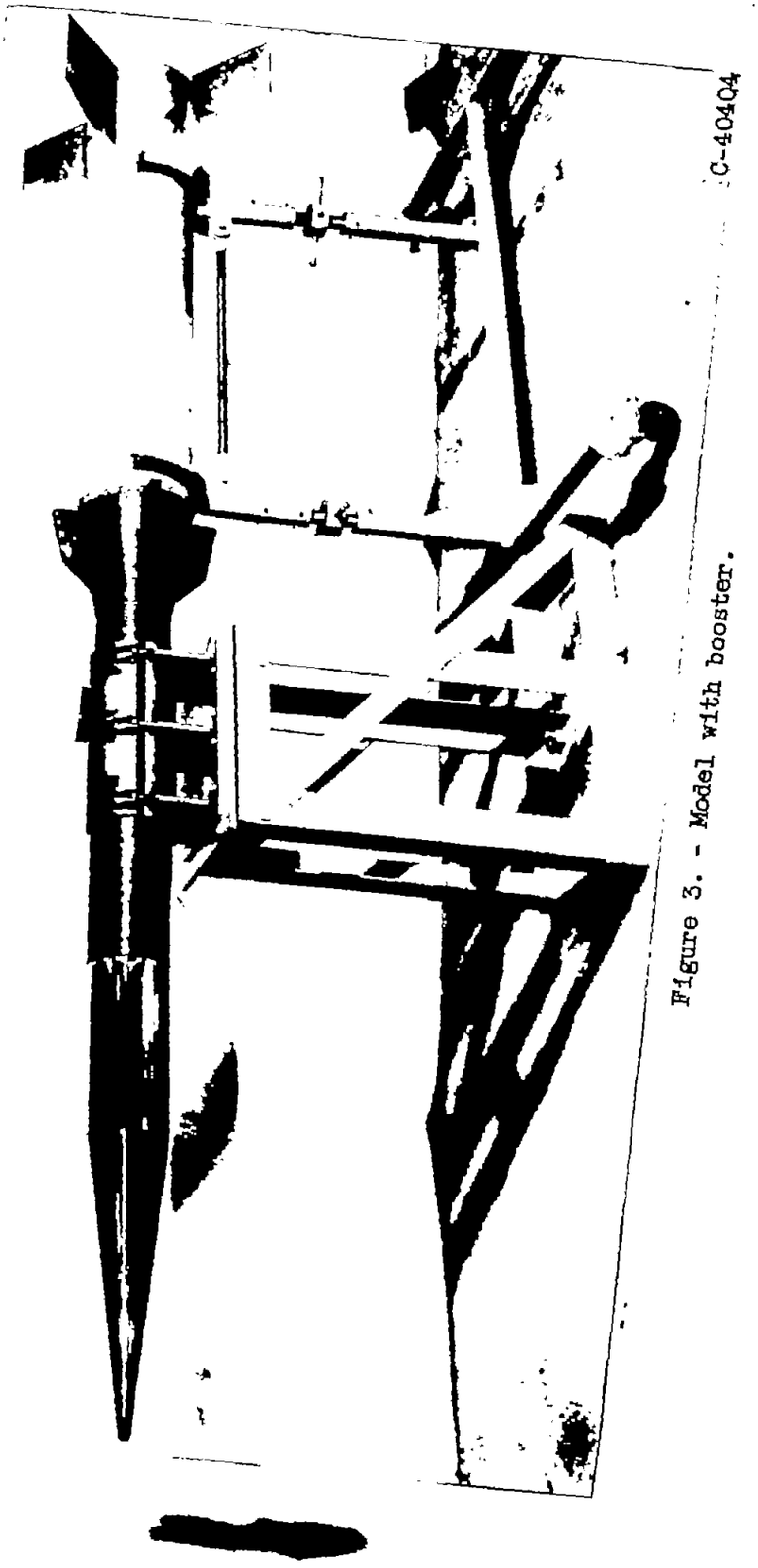

C-40404

Figure 3. - Model with booster.

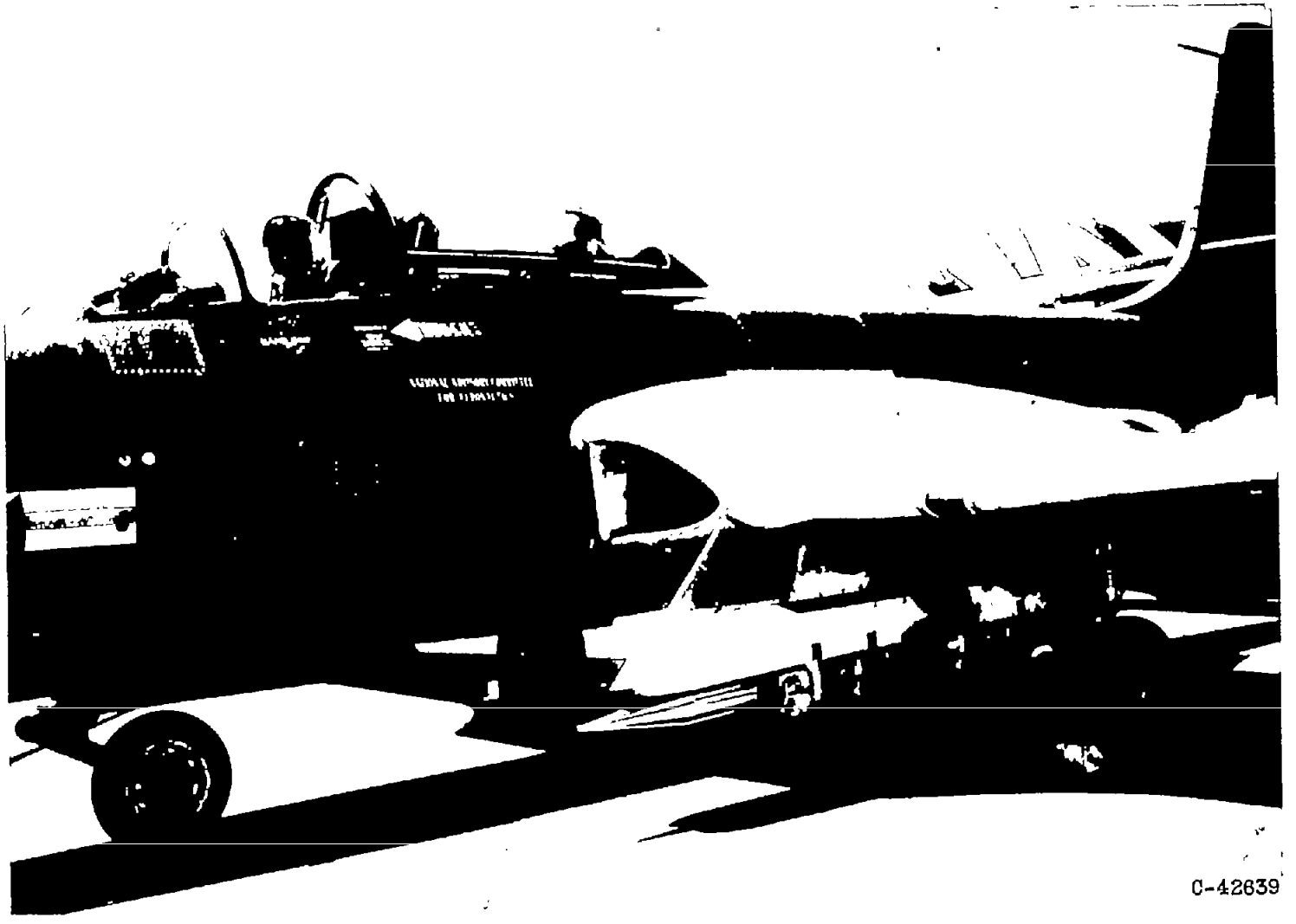

Figure 4. - Model mounted under F2H-2B airplane.

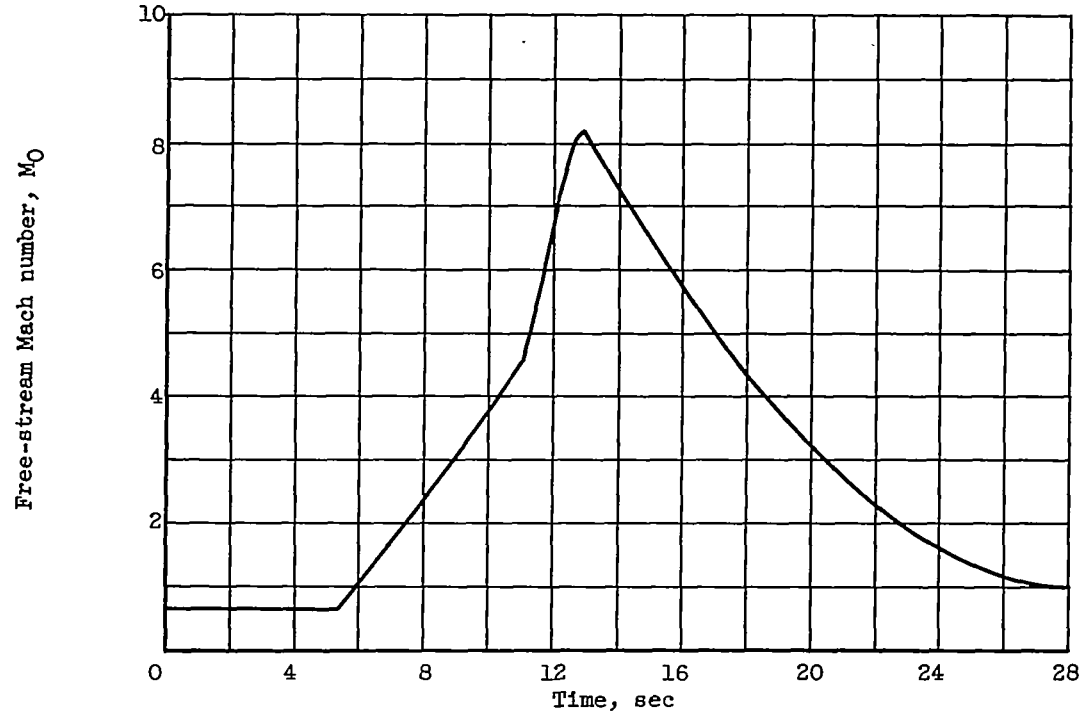

Figure 5. - Variation of free-stream Mach number with time.

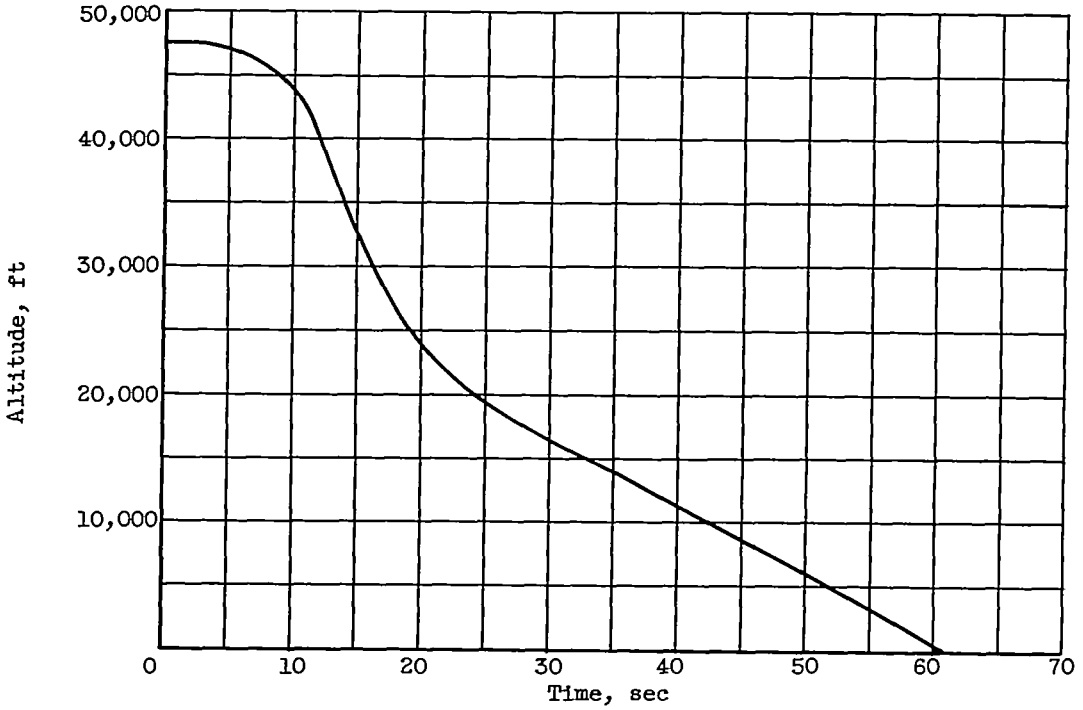

Figure 6. - Variation of altitude with time.

[redacted]

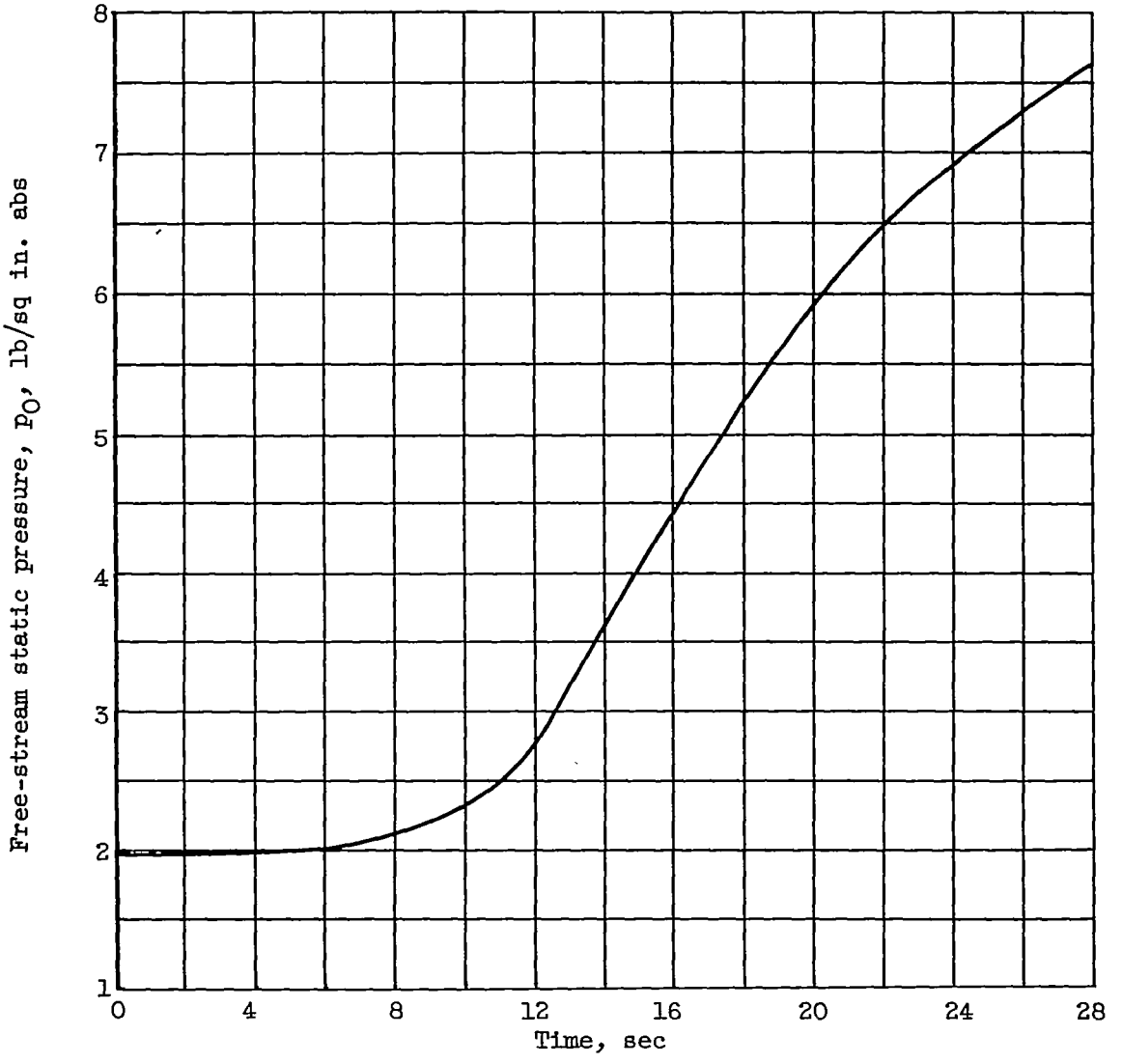

Figure 7. - Variation of free-stream static pressure with time.

[redacted]

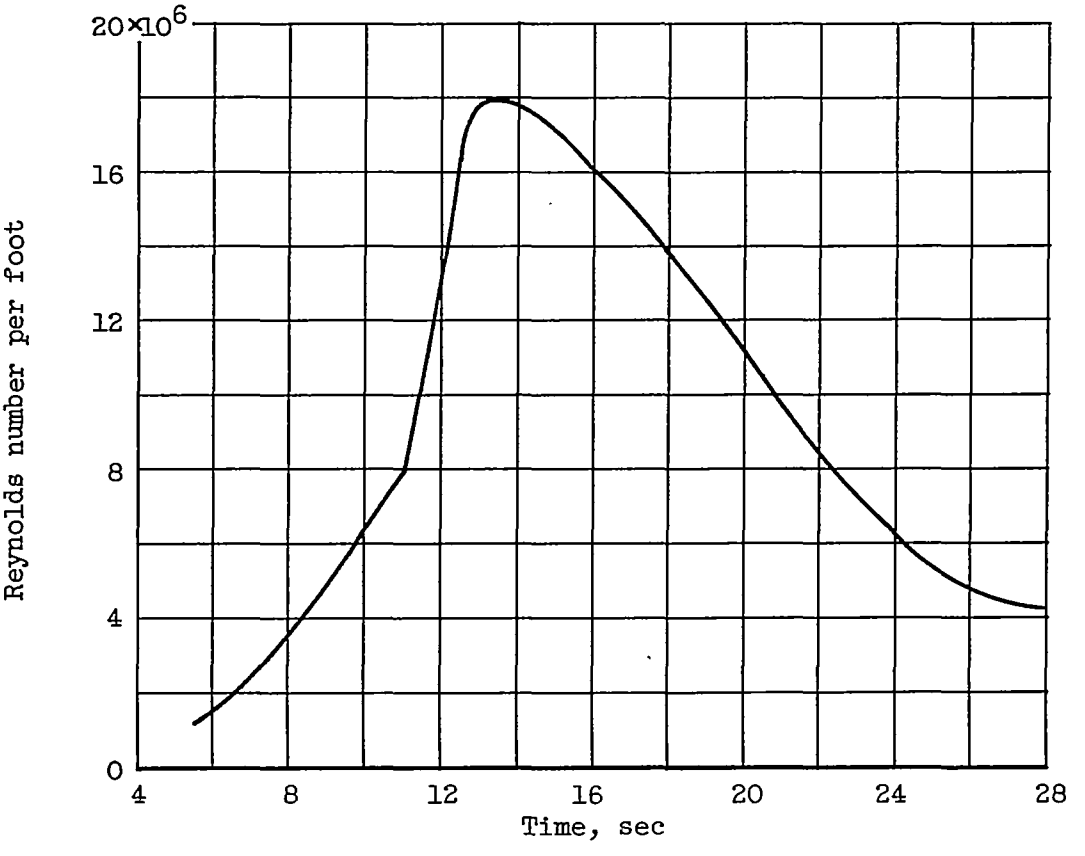

Figure 8. - Variation of free-stream Reynolds number per foot with time.

[redacted]

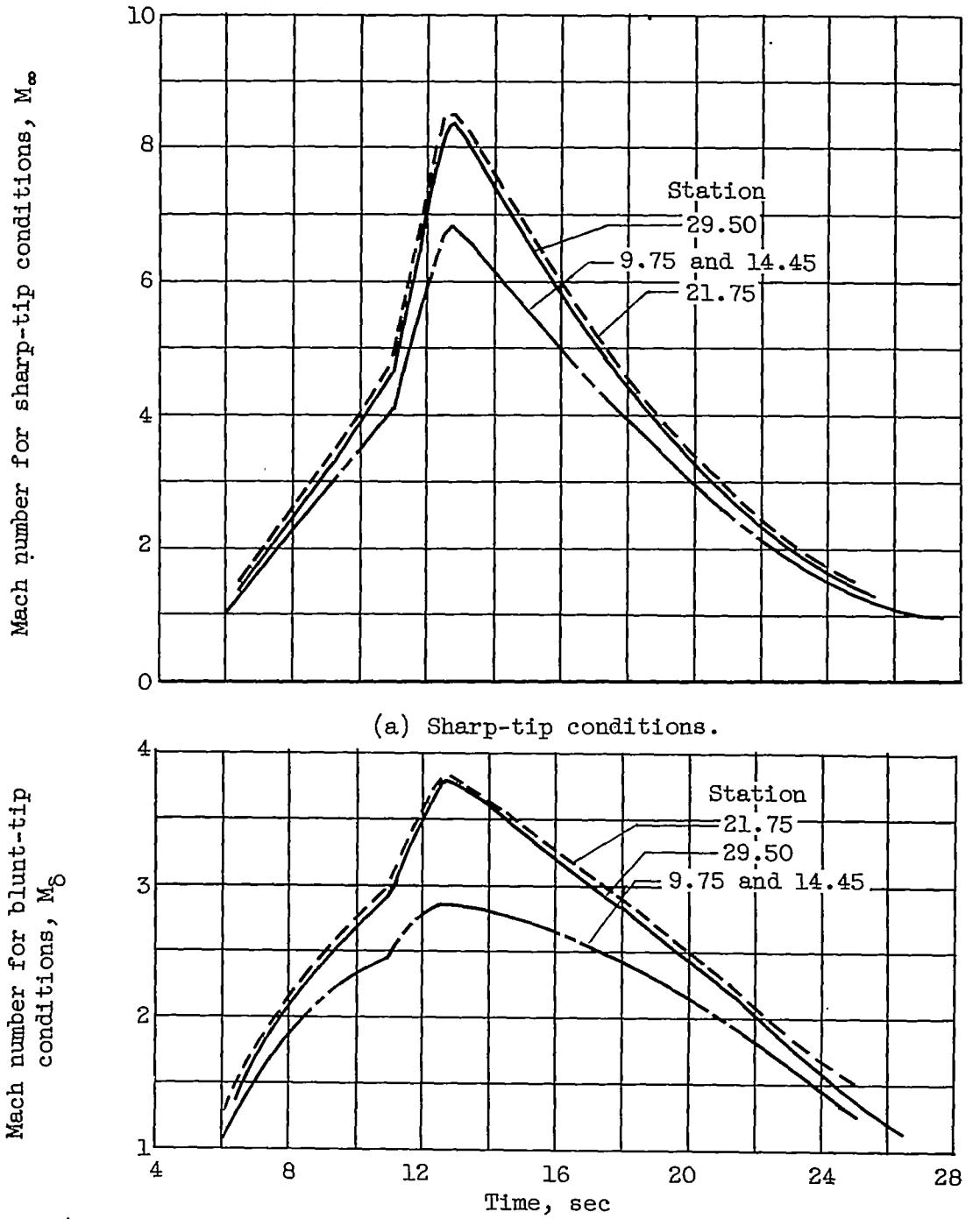

(a) Sharp-tip conditions.

(b) Blunt-tip conditions.

Figure 9. - Variation of Mach number outside boundary layer with time.

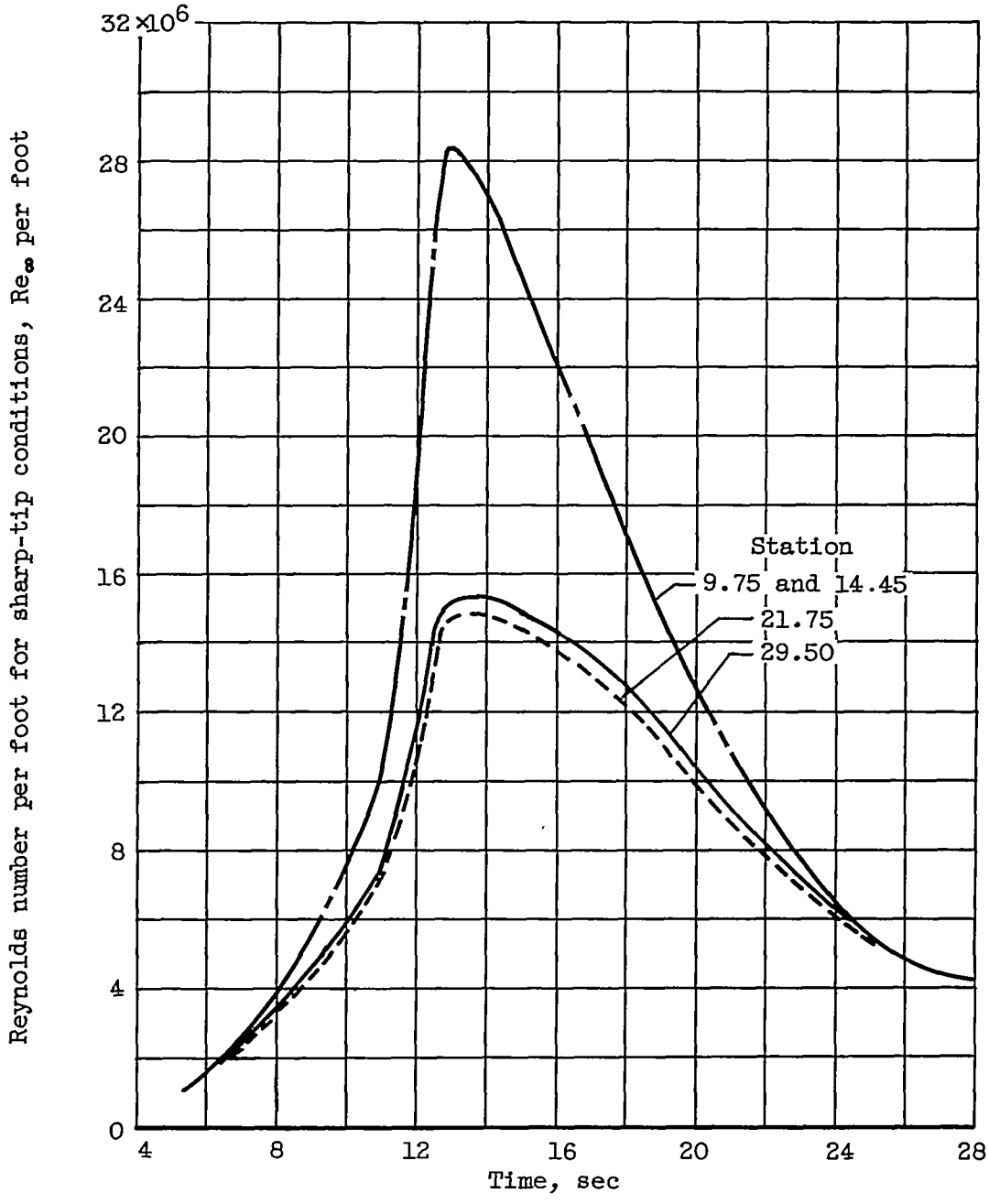

(a) Sharp-tip conditions.

Figure 10. - Variation of Reynolds number outside boundary layer with time.

[redacted]

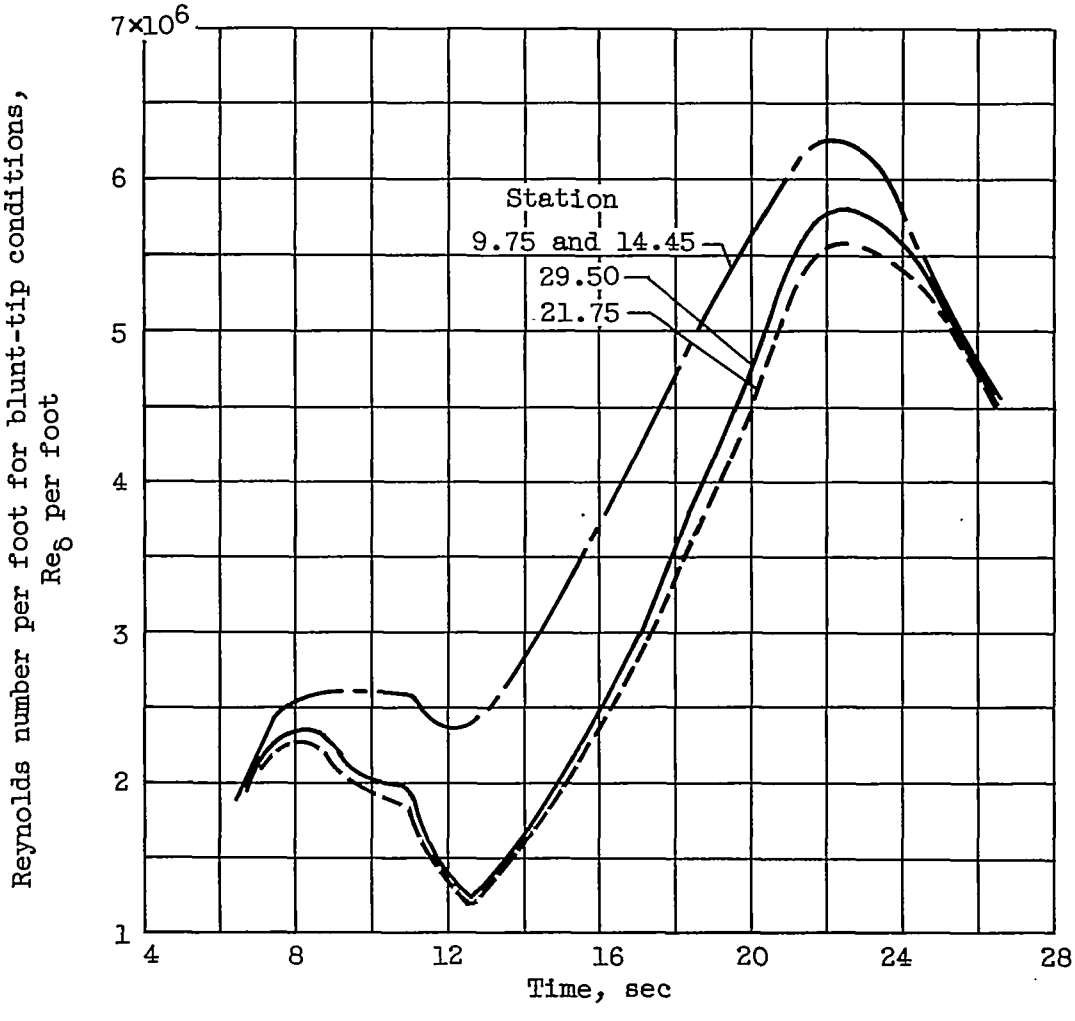

(b) Blunt-tip conditions.

Figure 10. - Concluded. Variation of Reynolds number outside boundary layer with time.

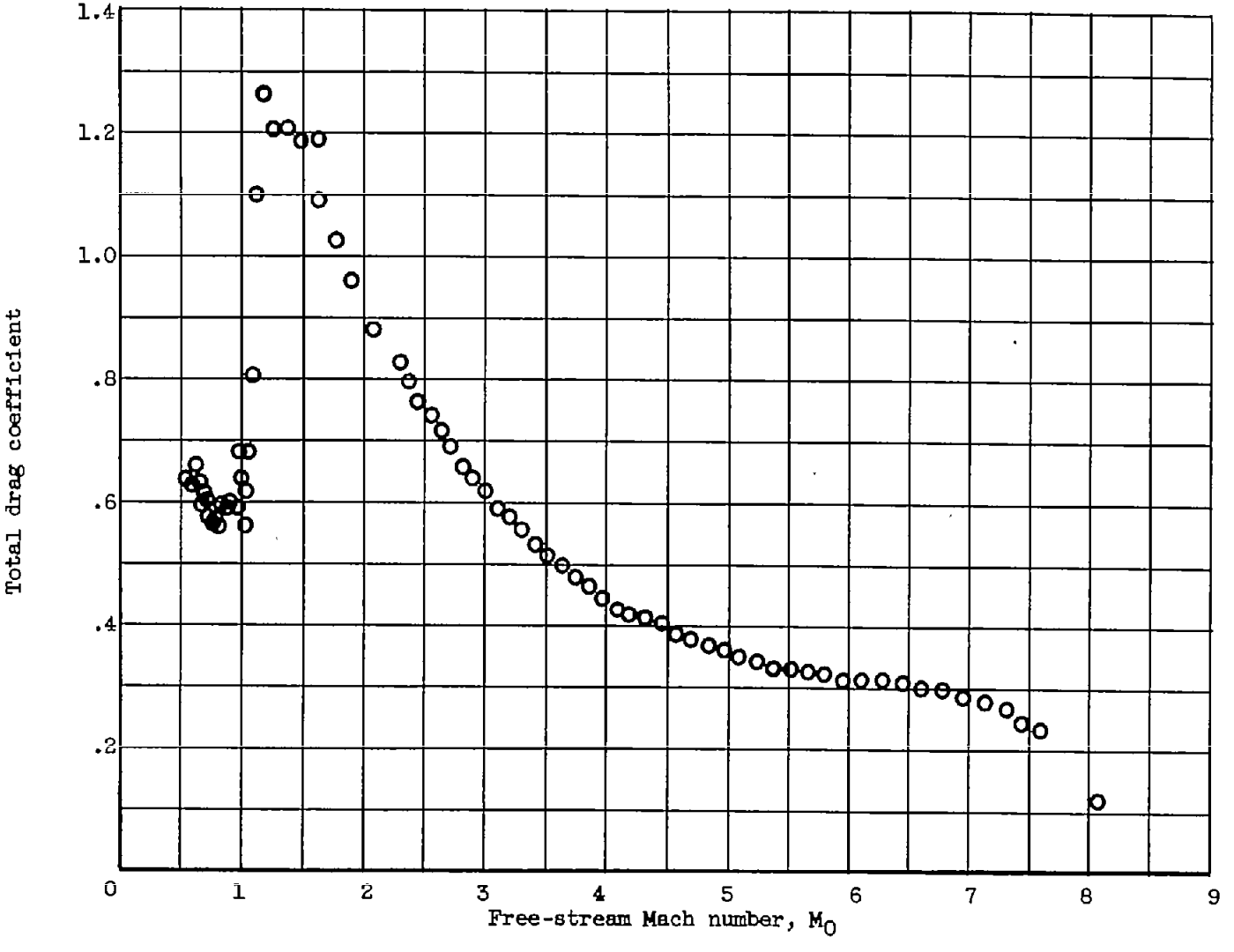

Figure 11. - Variation of total drag coefficient for sustainer stage with Mach number. Reference area, 0.196 square foot.

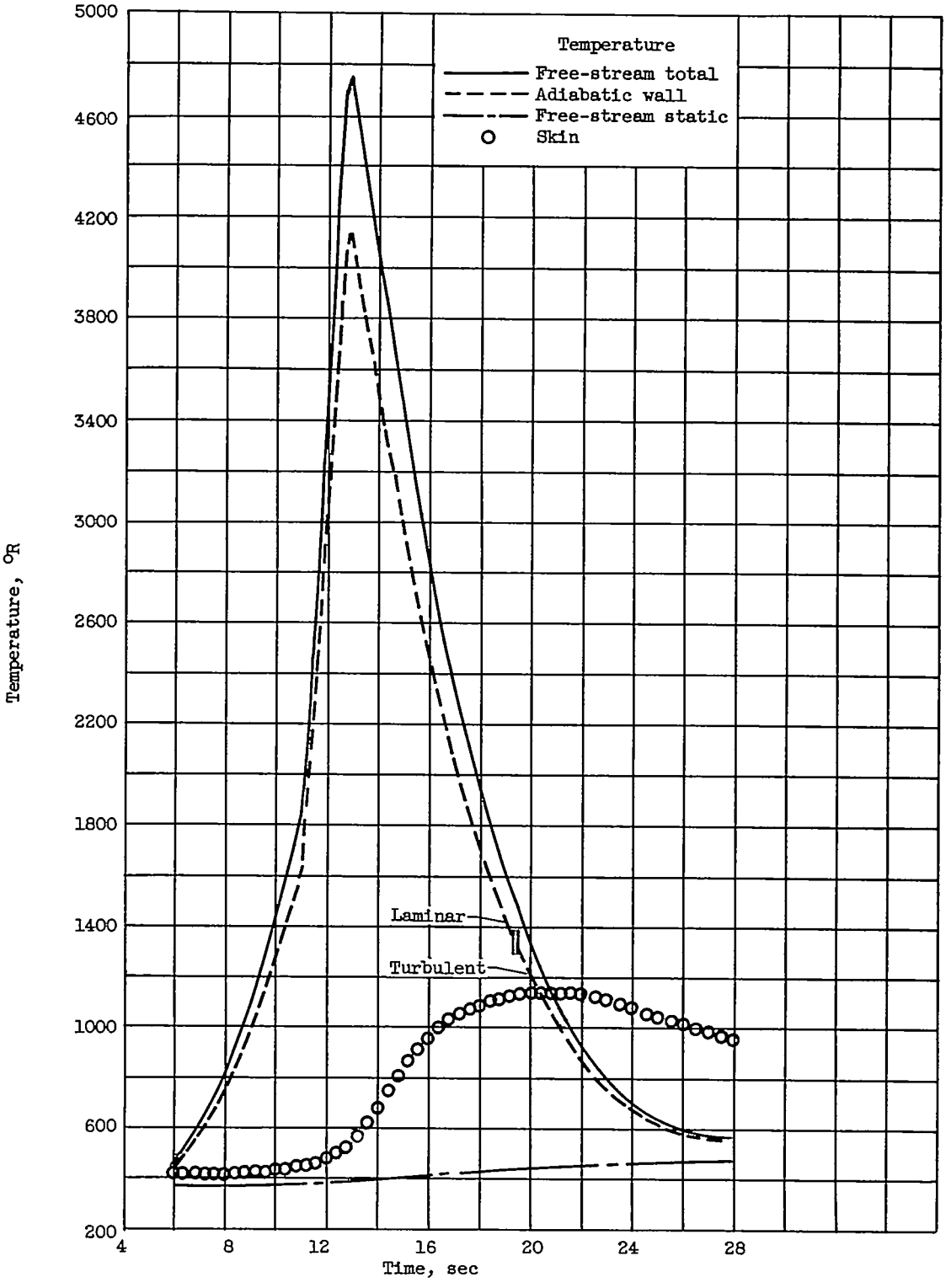

(a) Station 9.75.

Figure 12. - Variation of temperatures with time.

[redacted]

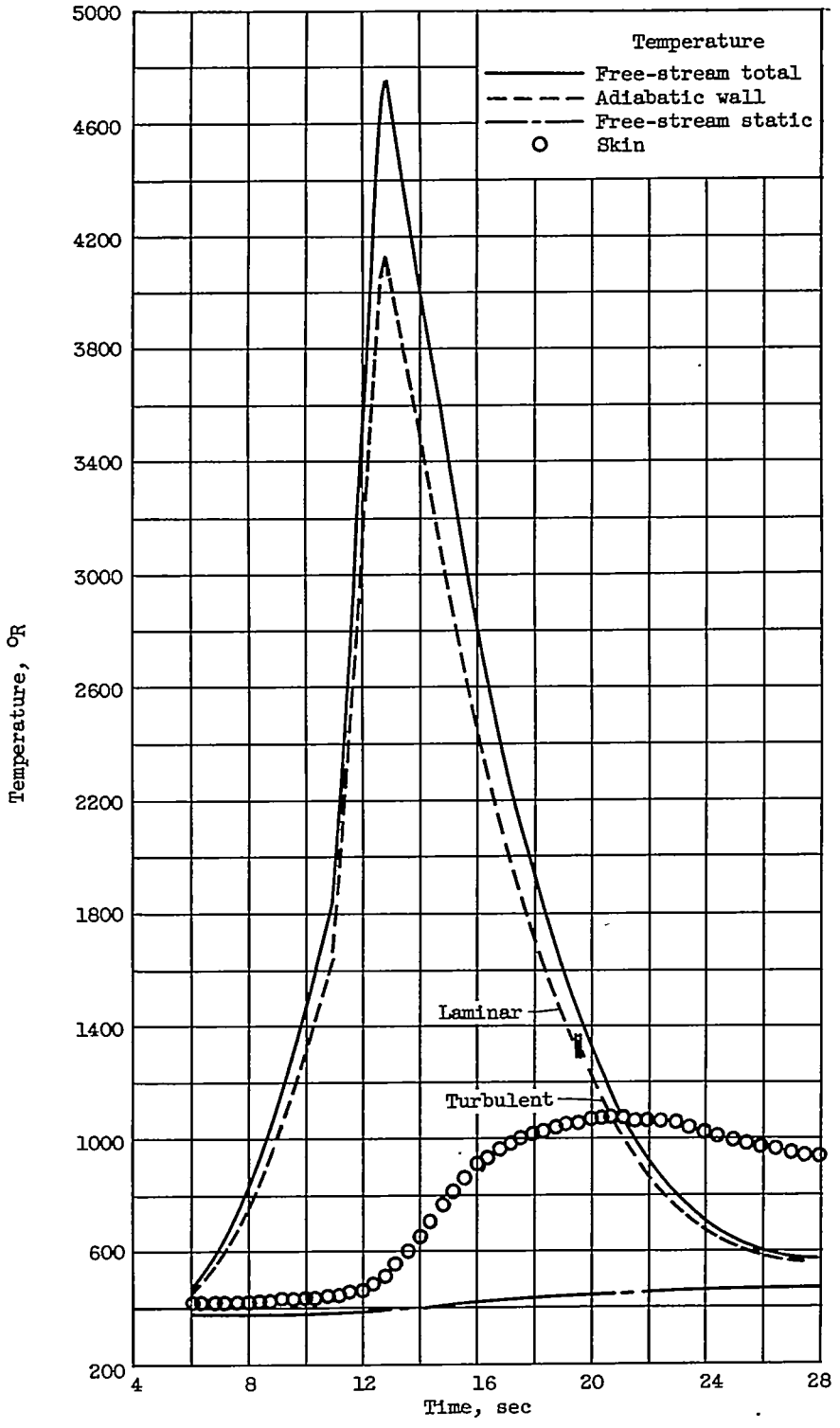

(b) Station 14.45.

Figure 12. - Continued. Variation of temperatures with time.

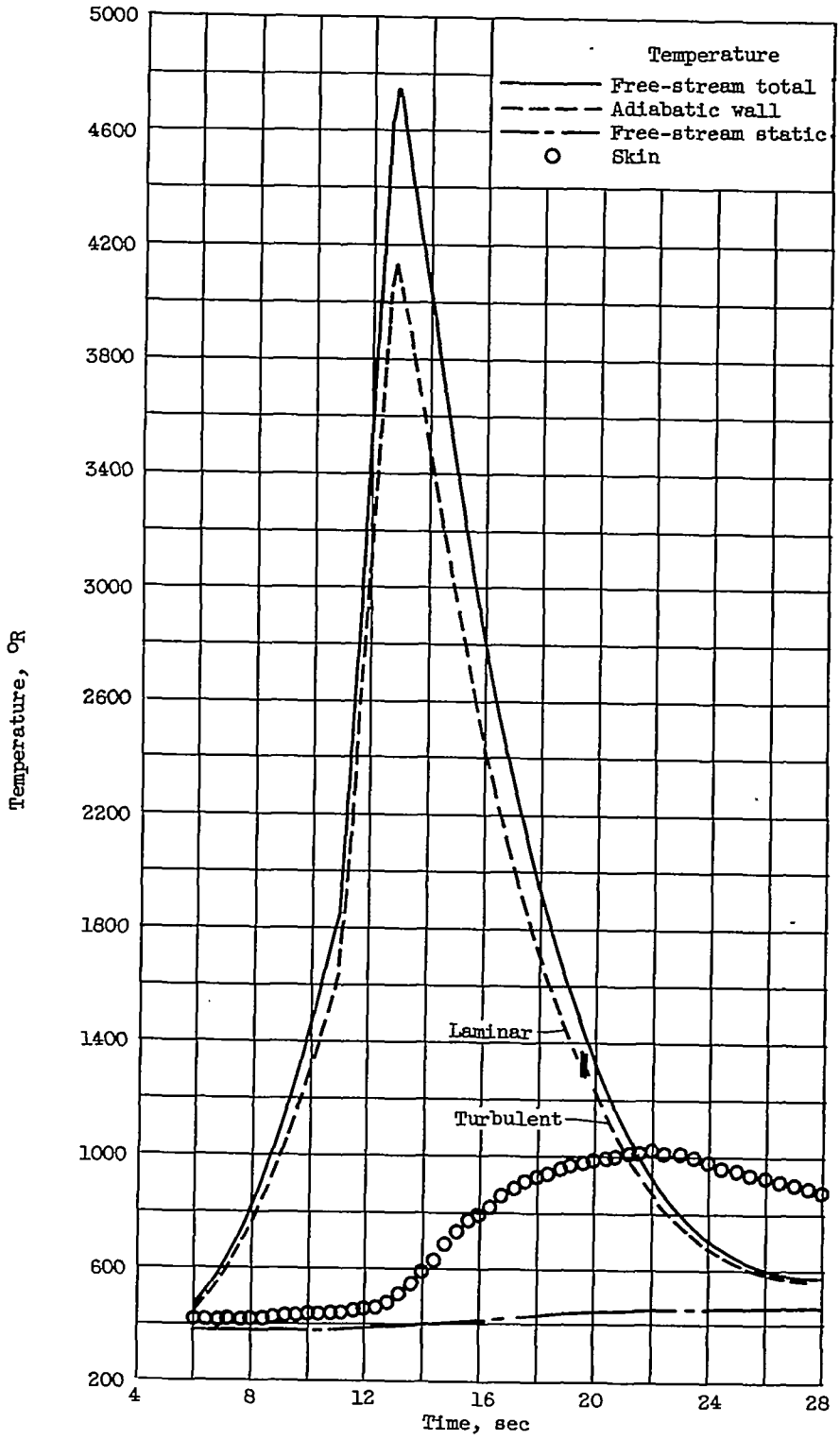

(c) Station 21.75.

Figure 12. - Continued. Variation of temperatures with time.

[redacted]

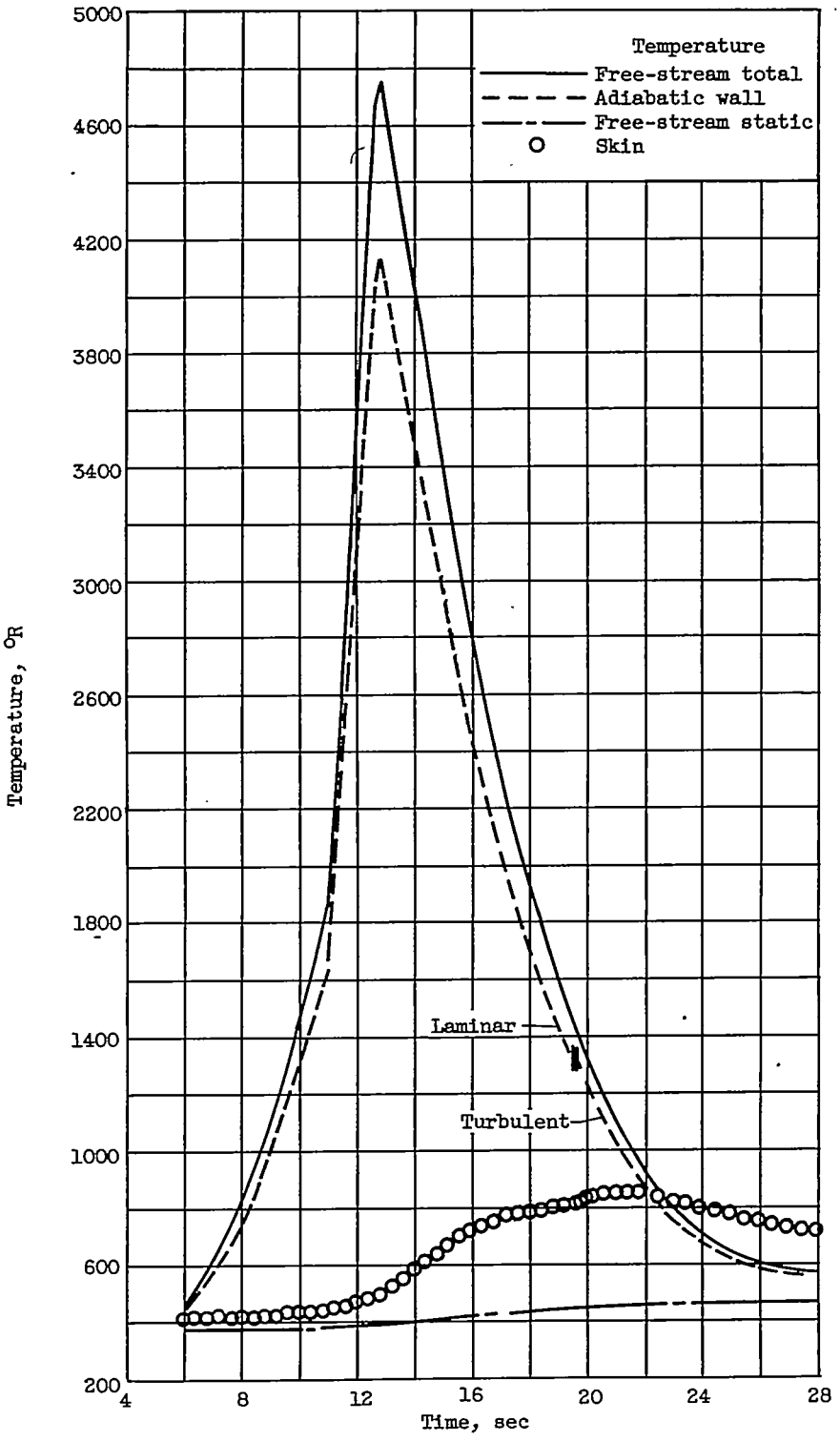

(d) Station 29.50.

Figure 12. - Concluded. Variation of temperatures with time.

[redacted]

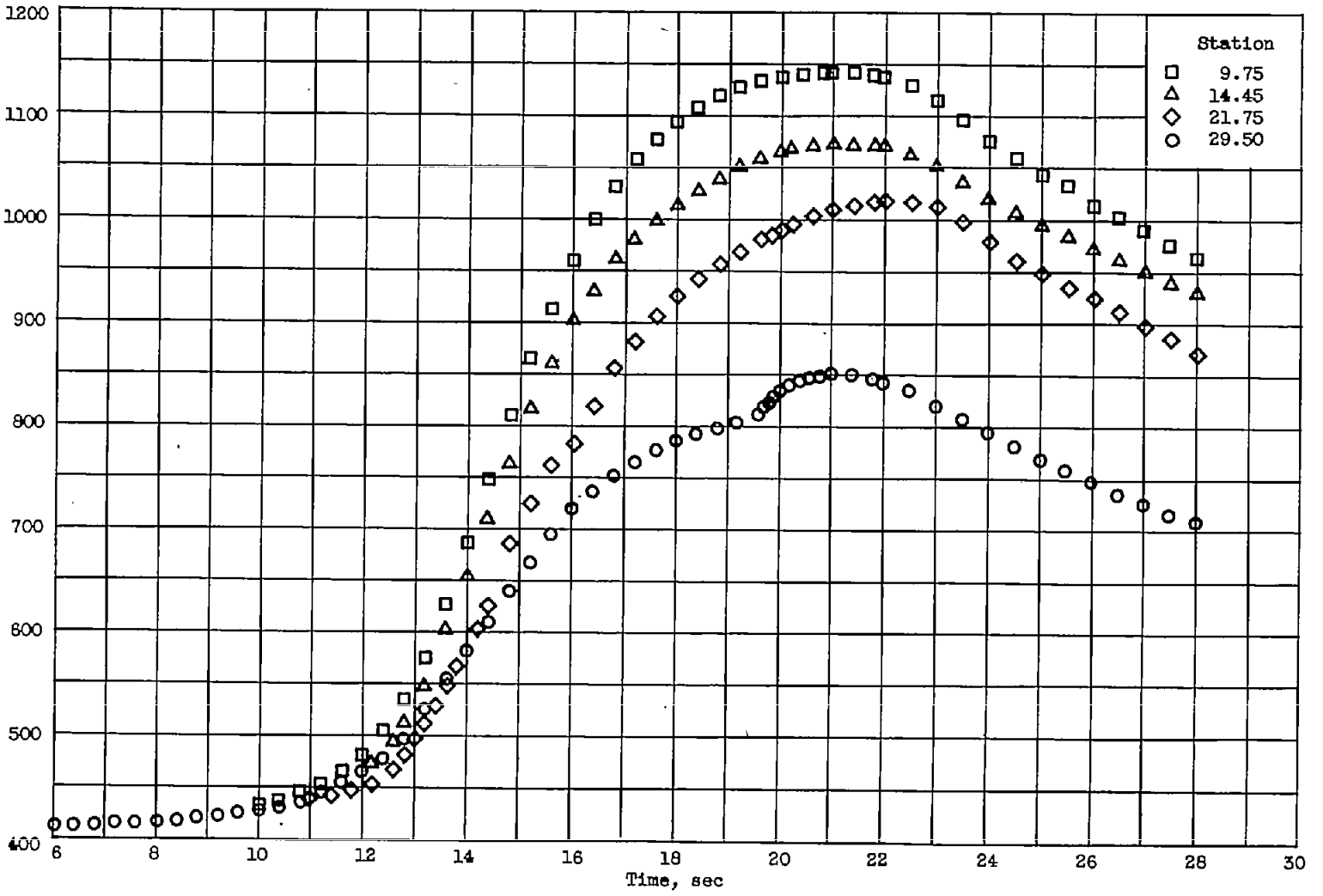

Figure 13. - Variation of skin temperatures with time.

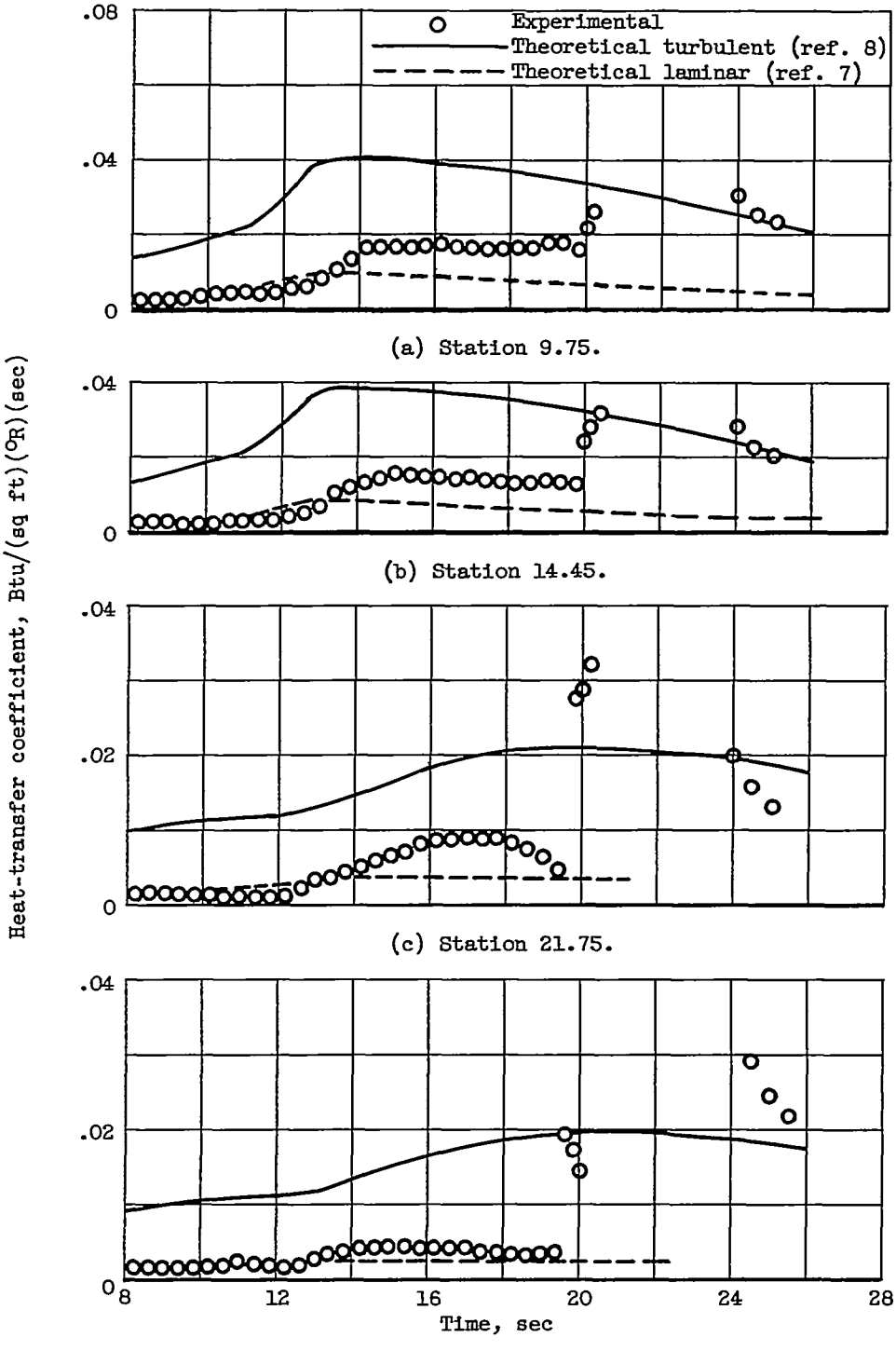

(a) Station 9.75.

(b) Station 14.45.

(c) Station 21.75.

(d) Station 29.50.

Figure 14. - Variation of heat-transfer coefficient with time. Blunt-tip conditions.

[redacted]

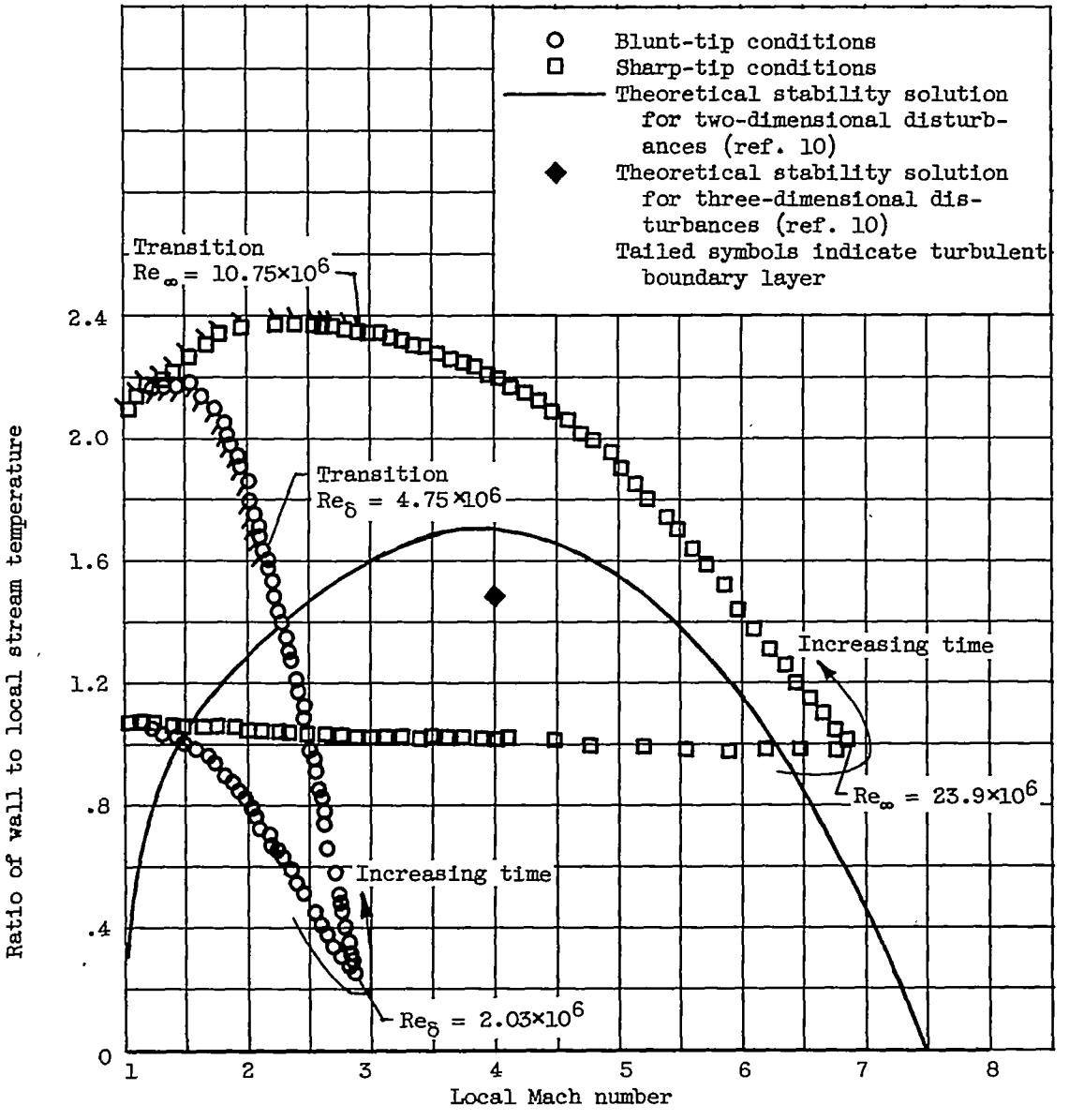

(a) Station 9.75.

Figure 15. - Variation of ratio of wall to local stream temperature with Mach number. Re_∞, Reynolds number for sharp-tip conditions; Re_δ, Reynolds number for blunt-tip conditions.

[redacted]

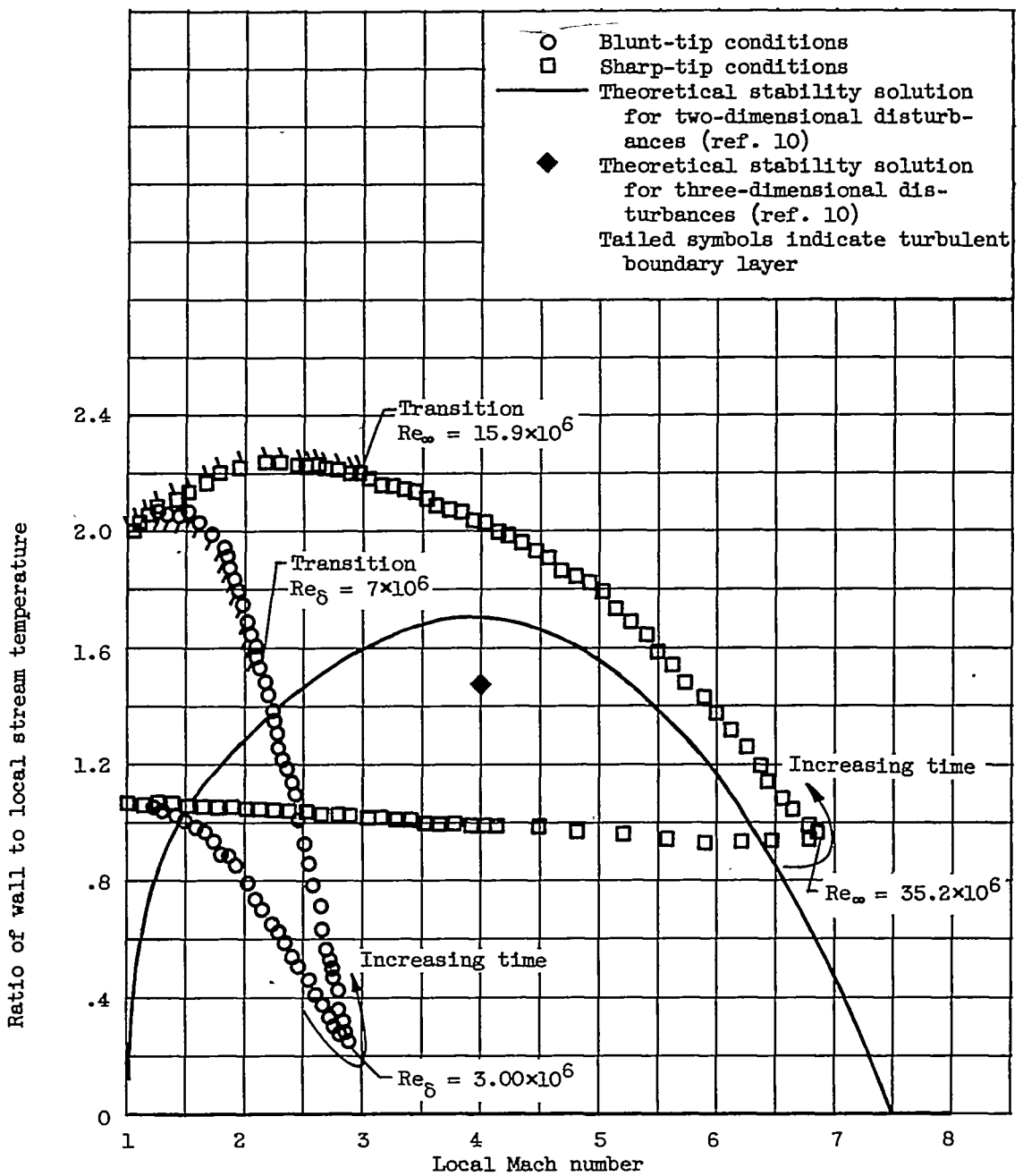

(b) Station 14.45.

Figure 15. - Continued. Variation of ratio of wall to local stream temperature with Mach number. Re_∞, Reynolds number for sharp-tip conditions; Re_δ, Reynolds number for blunt-tip conditions.

4048

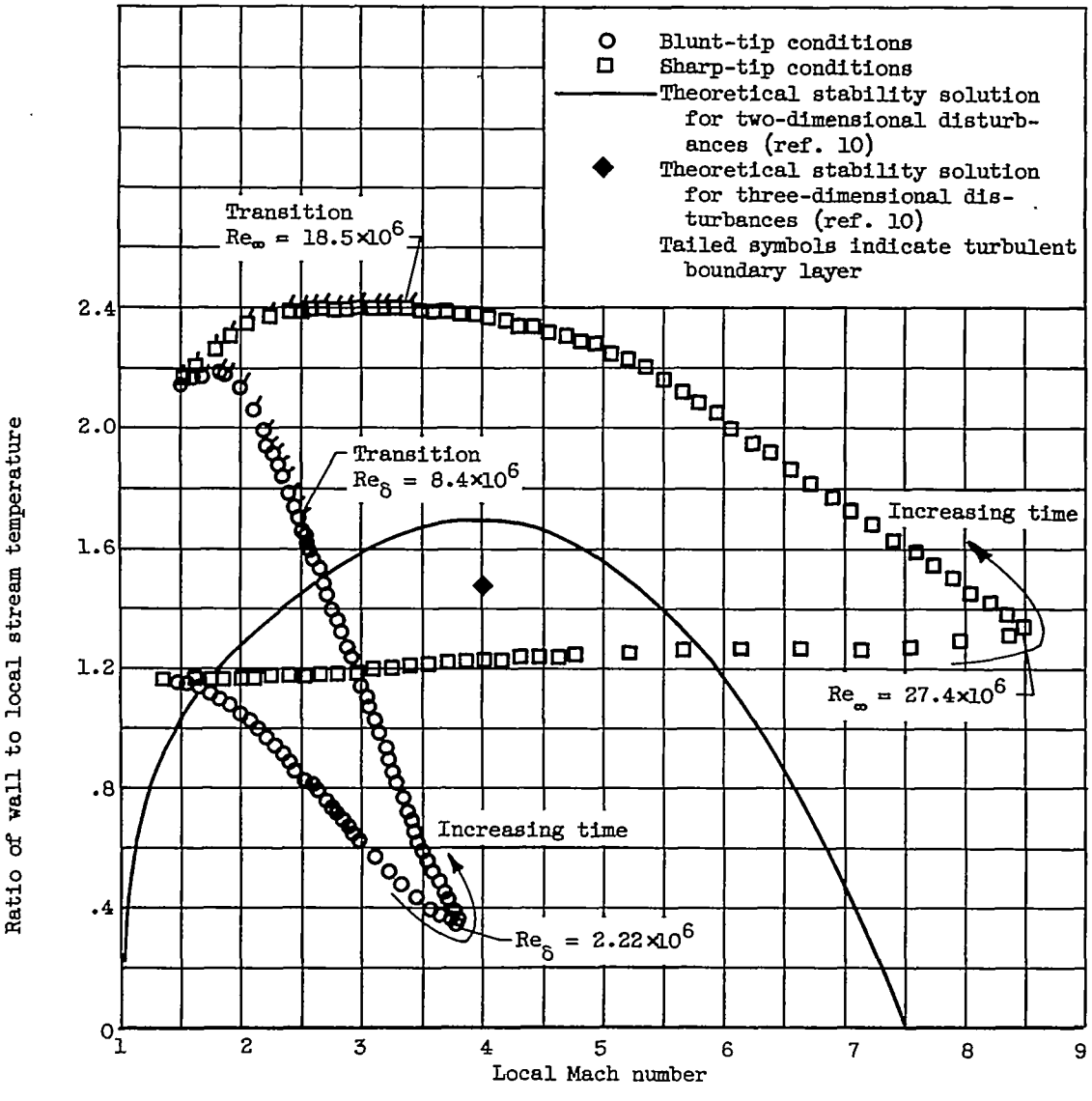

(c) Station 21.75.

Figure 15. - Continued. Variation of ratio of wall to local stream temperature with Mach number. Re_∞, Reynolds number for sharp-tip conditions; Re_δ, Reynolds number for blunt-tip conditions.

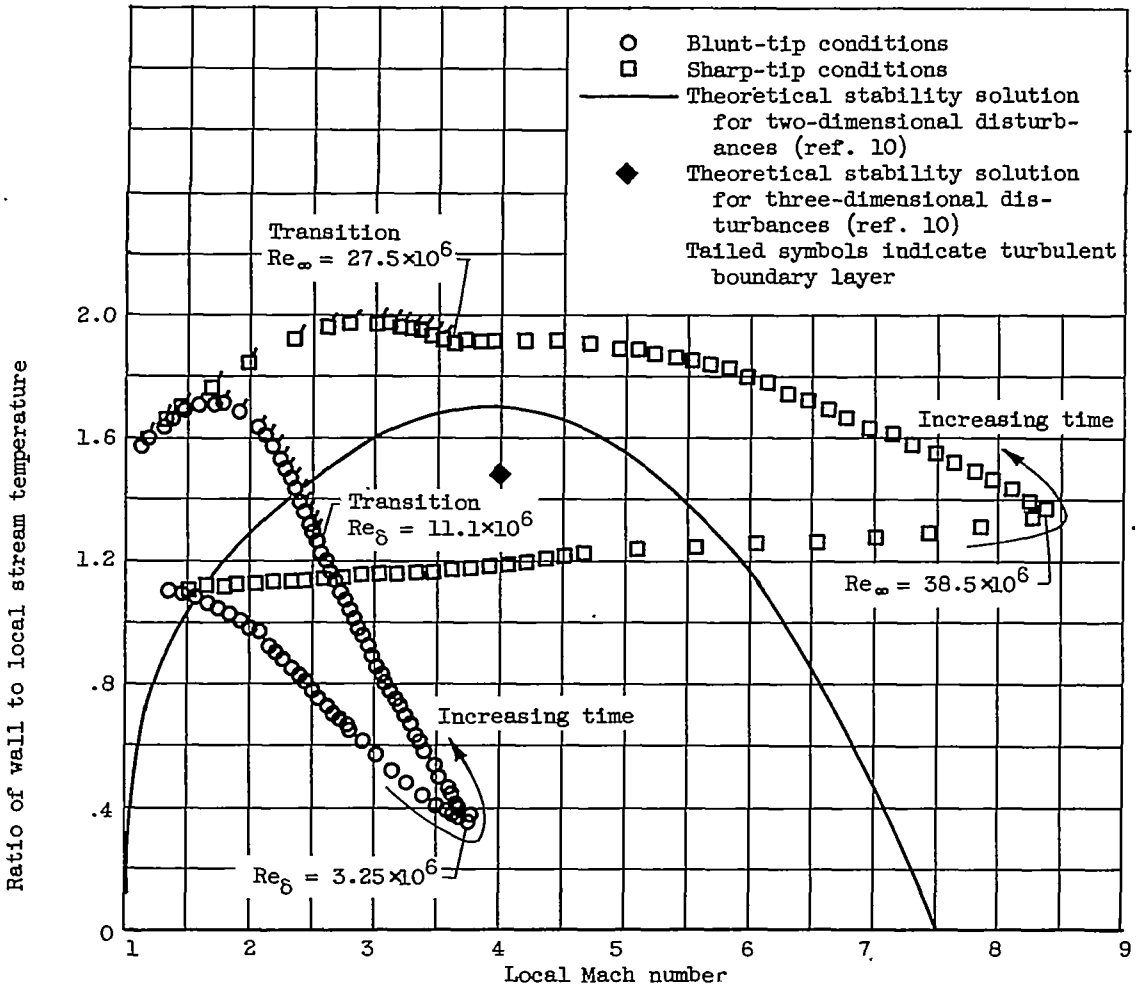

(d) Station 29.50.

Figure 15. - Concluded. Variation of ratio of wall to local stream temperature with Mach number. Re_∞, Reynolds number for sharp-tip conditions; Re_δ, Reynolds number for blunt-tip conditions.

[redacted]

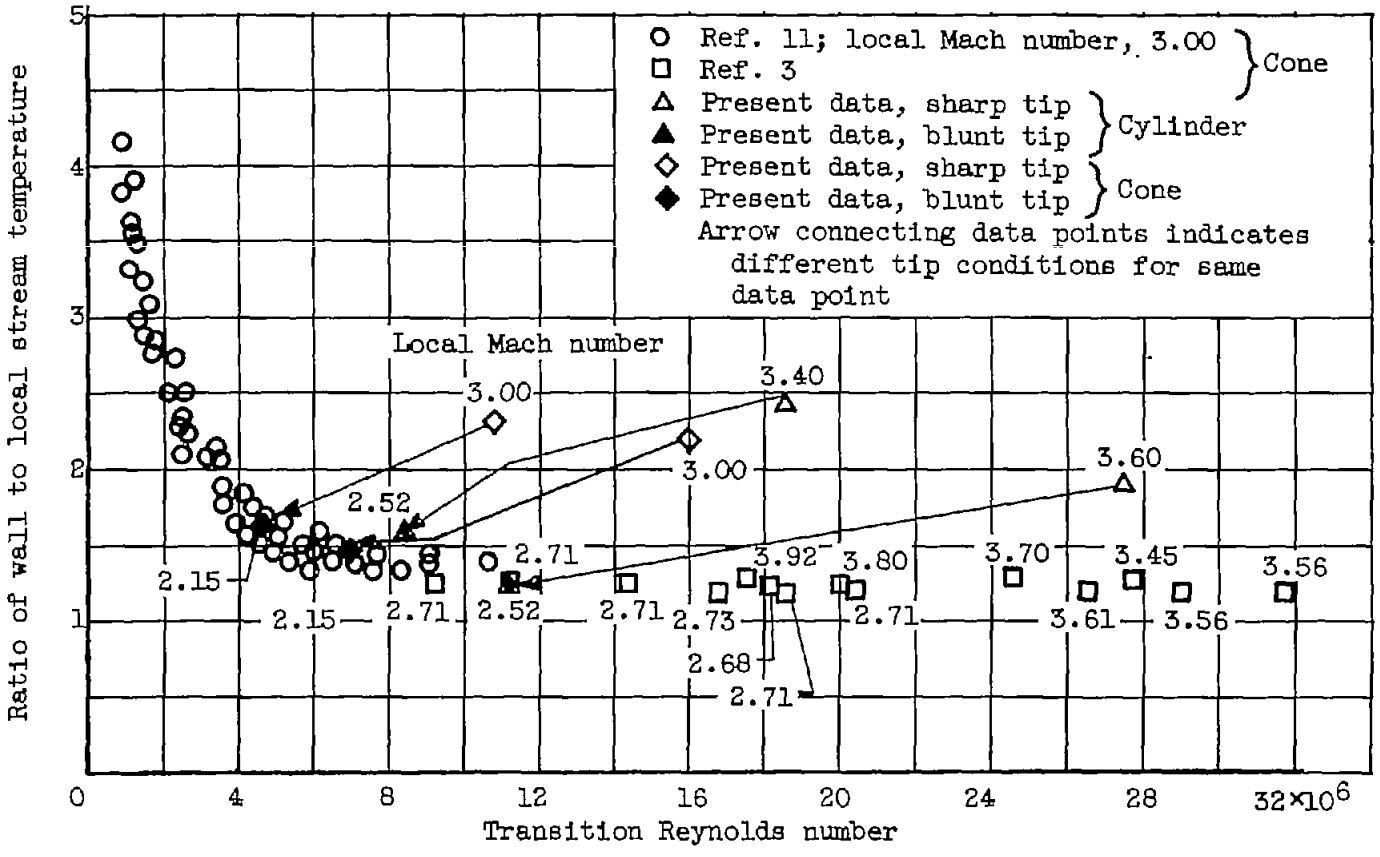

Figure 16. - Comparison of present data with previously obtained transition data for sharp-tipped cones.